A Computational Study of Complex Three-Dimensional Compressible Turbulent Flowfields

C. C. Horstman*
NASA Ames Research Center, Moffett Field, California

Abstract

A PARAMETRIC computational study is presented in which solutions of the time-dependent, Reynolds-averaged Navier-Stokes equations are compared with a family of experimental results for the three-dimensional interaction of a shock wave with a turbulent boundary layer. The solutions correctly predict the major features of the flowfield independent of the shock strength and extent of separation. The experimentally observed boundary between cylindrical and conical flow regimes is also predicted.

Contents

For the past few years, a class of three-dimensional shock/boundary-layer interactions generated by swept-back compression corners have been extensively studied.[1,2] For the flow geometry experimentally investigated (Fig. 1), the sweep-back angle λ was varied systematically from 0 deg (two-dimensional flow) to large values that produced highly separated three-dimensional flows for several values of the compression ramp angle α. It was found[1] that the resulting three-dimensional interactions exhibit either asymptotically cylindrical or asymptotically conical regimes, depending on the values of λ and α, but are independent of Reynolds number and the upstream boundary-layer thickness. The boundary between these two regimes (a function of λ and α) was experimentally determined at $M_\infty = 3$.

The partial differential equations used to describe the mean flowfield are the time-dependent, Reynolds-averaged Navier-Stokes equations for three-dimensional flow of a compressible fluid. For turbulence closure, the two-equation, k-ϵ, eddy viscosity model is used. The numerical procedure used here is the MacCormack's explicit second-order, predictor-corrector, finite-volume method modified by an efficient implicit algorithm. The computational domain (40 points in the streamwise direction, 26 points normal to the model surface, and 27 points in the crossflow direction) was varied in extent, depending on the size of the interaction. Typical streamwise grid spacings varied from 0.15 to 0.9 δ in the vicinity of the corner with the coarsest spacing for the largest interactions (high λ and α). By using two-dimensional wall-function boundary conditions[3] that have been adapted for three-dimensional flow, solutions were obtained in less than 30 min of CRAY-1S CPU time. Without the use of wall functions, the cases with the largest interaction zones would have required close to 4 hours of CPU time. This is because the maximum stable time step at which the code can be run is proportional to the minimum y-grid spacing, which is much larger when wall functions are used.

Thirty-five solutions for the swept compression corner have been obtained for various values of λ at $\alpha = 5$, 10, 16, 20, and 24 deg, duplicating the experimental test conditions described in Ref. 1. At each value of α, cylindrical flowfields were observed at low values of λ, and conical flowfields were observed at high values. Typical examples of these flowfields are depicted in Fig. 2, in which computed surface skin-friction lines are shown. The flowfields were determined from surface skin-friction line plots and surface pressure distributions (the same criteria used for the experimental study). Each computed surface skin-friction line pattern was examined for cylindrical or conical symmetry by fitting a straight line to the asymptotic locus of the upstream influence (L_m). If this line is parallel to the swept corner line (within narrow limits), then the upstream influence is asymptotically cylindrical. Divergence of these lines similarly denotes asymptotic conical flow. Computations were made through the boundary at constant α for increments in the sweep-back angle (λ) of 5 deg. Thus the computed boundary has a "width" of $\Delta\lambda = 5$ deg. The same procedure was used employing the computed pressure distributions that define the upstream influence as the location ahead of the corner where the pressure rise was 20% above the freestream pressure. The surface skin-friction line plots and pressure distributions gave the same location of the boundary. An excellent agreement is noted when, in Fig. 3, the experimental and computed results are compared. Also shown in Fig. 3 is the computed boundary between the attached and the separated flow which does not have any relationship with the cylindrical-conical boundary. The computed attached/separated flow boundary was determined from surface skin-friction line patterns. Separation is defined when the patterns show a convergence line that is ahead of the corner. The experimental results (not shown) for the attached/separated flow boundary are in good agreement with the computations.

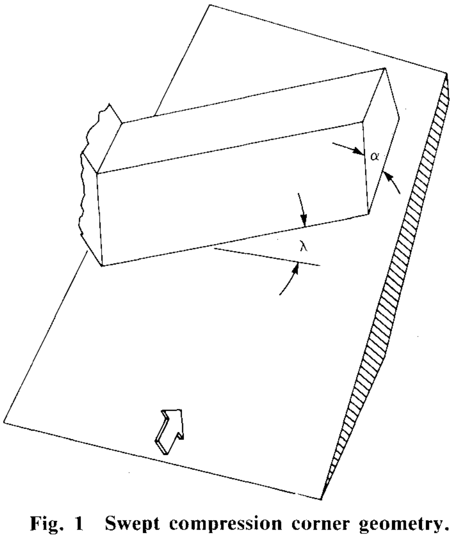

Fig. 1 Swept compression corner geometry.

Received March 26, 1984; presented as Paper 84-1556 at the AIAA 17th Fluid Dynamics, Plasma Dynamics, and Lasers Conference, Snowmass, Colo., June 25-28, 1984; revision received Nov. 20, 1984. Full paper available from AIAA Library, 555 W. 57th St., New York, N.Y. 10019. Price: microfiche, $4.00; hard copy, $9.00. **Remittance must accompany order.**

*Assistant Chief, Experimental Fluid Dynamics Branch. Associate Fellow AIAA.

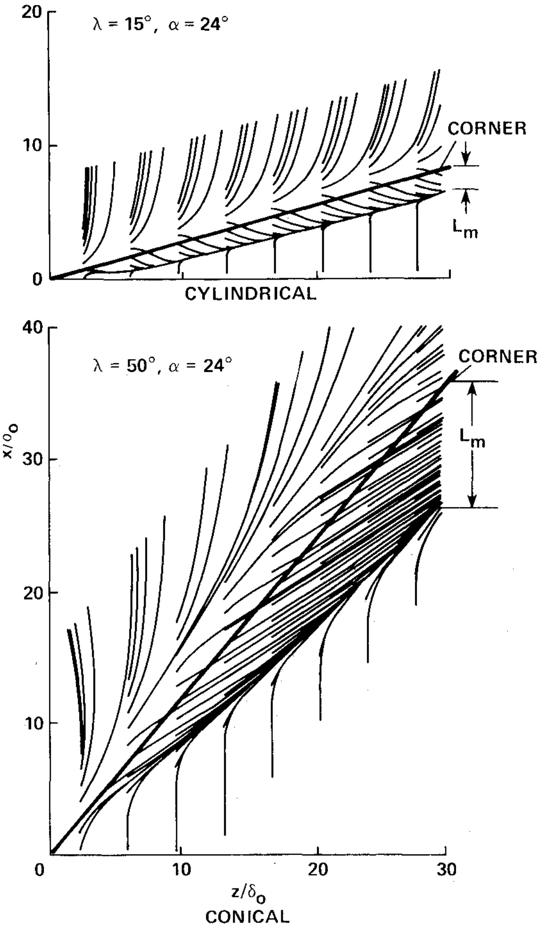

Fig. 2 Computed surface skin-friction lines.

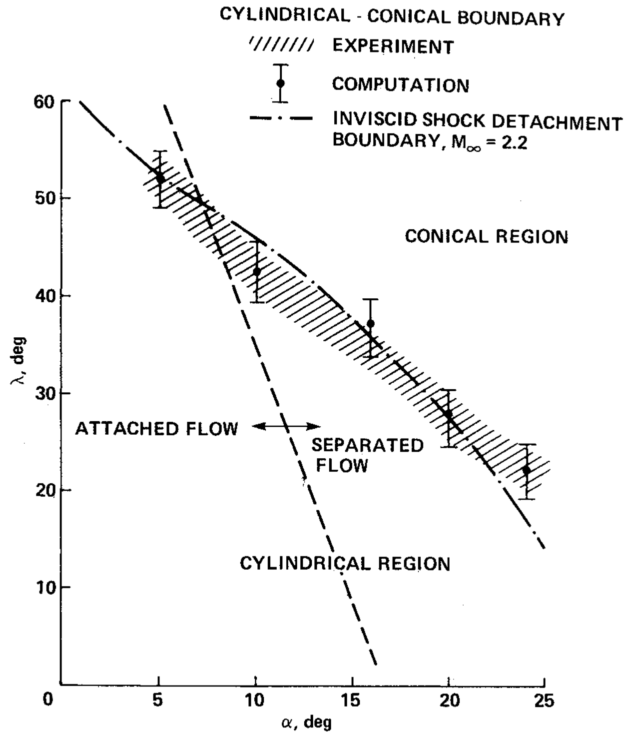

Fig. 3 The cylindrical/conical flow regime boundary—comparison of computations and experiment.

The authors of Ref. 1 postulated that the mechanism which determined the cylindrical/conical boundary was directly related to the phenomenon of inviscid shock detachment from a swept corner based on their experimental results. In fact, they found that the inviscid shock detachment boundary at $M_\infty = 2.2$ closely approximated their results. This boundary is shown in Fig. 3. The Mach number for detachment (2.2) is lower than the experimental freestream Mach number (3). This is a natural consequence of the fact that, because of the turbulent boundary layer, the true incoming flow of the experiments has a nonuniform Mach number distribution whose average value is lower than the freestream Mach number. Physically, this detachment hypothesis implies that the inviscid shock wave is a first-order determinant of upstream influence size and shape. It follows directly that cylindrical symmetry is associated with attached shocks and that conical symmetry is associated with detached shocks.

The present computations seem to confirm this detachment hypothesis. The calculated asymptotic values of the pressure ratio near the downstream boundary were compared with inviscid attached shock-wave pressure ratios for several values of α as a function of λ. The inviscid pressure ratios were computed using the freestream Mach number and compression corner angle normal to the swept corner. It was shown[4] that the computed downstream pressure ratio departs from the attached inviscid shock-wave value at the approximate location of the cylindrical/conical boundary for each value of α, indicating shock-wave detachment for conical flow regime. Computed shock-wave angles in a plane normal to the corner also indicated the same trends (i.e., the computed values deviate from the attached inviscid values near the location of the boundary). Further, various viscous phenomena such as separation or changes in the thickness of the initial boundary layer had no effect on this boundary. A few cases were calculated using an initial boundary-layer thickness increased by a factor of three for $\alpha = 24$ deg, but the resulting cylindrical/conical flow boundary remained unchanged (the same was shown experimentally in Ref. 1). This suggests that turbulence modeling, with the exception of determining the character of the incoming nonuniform boundary-layer profile, does not play a significant role in the location of this boundary.

Comparisons between experimental and computed surface pressure distribution and upstream influence distances are given in Ref. 4.

The computations have shown both cylindrical and conical flowfields. The computed boundary between these flow regimes agreed with experimental measurements. The location of this boundary was shown to be basically an inviscid phenomenon directly related to shock-wave detachment. The experimental shape and location of cylindrical/conical boundary was the result of a family of experiments rather than an isolated test. More confidence in the computations giving the correct physics of the flowfields was gained since the parametric study predicted the experimental trends as opposed to a comparison between measured and computed results for an isolated test case.

References

[1]Settles, G. S. and Teng, H. Y., "Cylindrical and Conical Upstream Influence Regimes of Three-Dimensional Shock/Turbulent Boundary Layer Interactions," *AIAA Journal*, Vol. 22, Feb. 1984, pp. 194-200.

[2]Settles, G. S. and Bogdonoff, S. M., "Scaling of Two- and Three-Dimensional Shock/Turbulent Boundary Layer Interactions at Compression Corners," *AIAA Journal*, Vol. 20, June 1982, pp. 782-789.

[3]Viegas, J. R. and Rubesin, M. W., "Wall-Function Boundary Conditions in the Solution of the Navier-Stokes Equations for Complex Compressible Flows," AIAA Paper 83-1694, July 1983.

[4]Horstman, C. C., "A Computational Study of Complex Three-Dimensional Compressible Turbulent Flow Fields," AIAA Paper 84-1556, June 1984.